J Mol Model (2011) 17:2609–2621
DOI 10.1007/s00894-011-0956-0

ORIGINAL PAPER

Hydrogen bonding interactions in noradrenaline-DMSO complexes: DFT and QTAIM studies of structure, properties and topology

Zhengguo Huang · Yumei Dai · Lei Yu · Hongke Wang

Received: 4 October 2010 / Accepted: 3 January 2011 / Published online: 22 January 2011

Abstract The hydrogen bonding interactions between noradrenaline (NA) and DMSO were studied with density functional theory (DFT) regarding their geometries, energies, vibrational frequencies, and topological features of the electron density. The quantum theory of atoms in molecules (QTAIM) and the natural bond orbital (NBO) analyses were employed to elucidate the hydrogen bonding interaction characteristics in noradrenaline-DMSO complexes. The H-bonds involving the hydroxyls hydrogen in NA and the O atom in DMSO are dominant intermolecular H-bonds and are stronger than other H-bonds involving the methyl hydrogen of DMSO as a H-donor. The weak H-bonds also include a π H-bond which involves the benzene ring as a H-donor or H-acceptor. QTAIM identified the weak H-bonds formed between the methyl hydrogen of DMSO and the N atom in NA in some complexes (**AB5**, **AB6** and **AB7**), which cannot be further confirmed by NBO and other methods, so there are probably no interactions between hydrogen and nitrogen atoms among these complexes. A good linear relationship between logarithmic electron density ($\ln\rho_b$) at the bond critical point (BCP) and structural parameter ($\delta R_{H\cdots Y}$) was found. The formations of new H-bonds in some complexes are helpful to strengthen the original intramolecular H-bond, this is attributed to the cooperativity of H-bonds in complexes and can be learned from the structure results and the NBO and QTAIM analyses. Analysis of various physically meaningful contributions arising from the energy decomposition procedures show that the orbital interactions of H-bond is predominant during the formation of the complex, moreover, both the hydrogen bonding interaction and the structural deformation are responsible for the stability of the complexes.

Keywords Density functional theory (DFT) · DMSO · Hydrogen bond · Natural bond orbital (NBO) · Noradrenaline · Quantum theory of atoms in molecules (QTAIM)

Z. Huang (✉) · Y. Dai · L. Yu · H. Wang
Tianjin Key Laboratory of Structure and Performance
for Functional Molecule, College of Chemistry,
Tianjin Normal University,
Tianjin 300387, People's Republic of China
e-mail: hsxyhzg@126.com

Introduction

Noradrenaline (NA) is the simplest member of the catecholamine series of neurotransmitters and is widely distributed in various organisms. NA plays an important role in biological systems since it controls a wide variety of physiological and behavioral processes mainly through different receptor types. Like other amine neurotransmitters (such as dopamine, adrenaline and serotonin), NA is electroactive, so that it can be monitored electrochemically. The electrochemical behavior of NA have been the topic of very interesting studies in the past decades [1–9]. The electrochemical behavior of NA is affected by solvents, especially by polar aprotic solvents because of the formation of hydrogen bonding interactions between solvents and NA. For example, experimental and theoretical research on the conformations of NA in the gas phase and in aqueous solution has shown that the preferred conformations in solution differ markedly from those of their neutral or protonated counterparts [10–15]. However, the solvent effects on the structure and properties of NA have received comparatively little attention. Therefore, it would be of interest to study the interactions between different solvents and NA.

Dimethyl sulfoxide (DMSO) is a typical polar aprotic solvent which can dissolve both polar and nonpolar compounds and is miscible in a wide range of organic solvents as well as water. Previous studies showed that DMSO can prevent the electrochemical oxidization of adrenaline by forming H-bonds [16, 17]. Although NA and adrenaline have similar structures, however, NA has one chiral center (the side chain carbon atom bearing four different groups). Therefore, the interactions between NA and DMSO should be different from those between adrenaline and DMSO. The hydrogen bonding interaction is believed to be the dominant interaction between neurotransmitters and DMSO. Therefore, the aim of this paper is to study the hydrogen bonding interactions between NA and DMSO by theoretical chemistry methods. Our previous researches [16–19] showed that the hydrogen bonding interactions are very complicated even in such simplified model systems because more than one proton donor (H-donor) and acceptor (H-acceptor) sites can be found in NA or DMSO molecule. The MP2 method is reliable to characterize the nature of a H-bond. However, it is not a cost-effective approach for such biomolecular systems even with a medium-size basis set. On the other hand, conventional density functional theory (DFT) cannot better describe hydrogen bonding interactions although it has been accepted as a cost-effective approach (e.g., see refs. [20, 21] and references therein). Recently, many functionals (such as B2PLYP [22], M06L [23, 24] and ωB97XD [25]) have been developed to treat hydrogen bonding and van der Waals interactions within DFT. These range from physically rigorous dispersion functionals derived from first principles to entirely empirical corrections or parameterizations. A comprehensive review of such methods is given by Johnson et al. [26]. Many studies have shown that these new DFT methods can give reliable results for a wide variety of weakly bonded systems [22, 27–29]. In addition, the quantum theory of atoms in molecules (QTAIM) [30–32] and the natural bond orbital (NBO) analysis [33, 34] have been proven to be very useful tools in understanding of H-bonds. In this study, we mainly discuss the structures and hydrogen bonding interactions of the NA-DMSO complexes by DFT calculations, QTAIM and NBO analyses are carried out to study the nature of H-bonds.

Computational details

In this paper, the ωB97XD functional [25] with the 6-311++G(d,p) basis set [35, 36] was used. The ωB97XD functional includes empirical dispersion and can better treat hydrogen bonding and van der Waals interactions than conventional DFT functionals. First, the geometries of the isolated NA and DMSO monomers were fully optimized. The complexes were constructed starting from the most stable NA and DMSO monomers. All complexes were also fully optimized at the same level. The counterpoise (CP) correction [37] was implemented in each step of the iterative process of geometry optimization in an integrated way in order to ensure that complexes and monomers are being computed with a consistent basis set. The harmonic vibrational frequencies were calculated with analytic second derivatives at the ωB97XD/6-311++G(d,p) level as well, which confirm the structures as minima and enable the evaluation of zero-point vibrational energies (ZPVE). All ZPVE and frequencies were unscaled. Finally, the interaction energies were calculated based on the ZPVE and BSSE corrections. The QTAIM and the NBO analyses were also implemented to provide complementary information on the H-bond. All DFT calculations and NBO analyses were performed with the Gaussian09 [38]. The QTAIM analysis were carried out by using the software AIM2000 [39] with ωB97XD wave functions employing the 6-311++G(d,p) basis set.

Results and discussion

Recently, conformers of NA have been studied by different research groups [11–13, 40–42]. In this work, the structure of isolated NA was well reproduced at the ωB97XD/6-311++G (d,p) level. The optimized conformers of NA (A) and DMSO (B) were presented in Fig. 1. As shown in Fig. 1, NA and DMSO molecules can offer several possible donor and

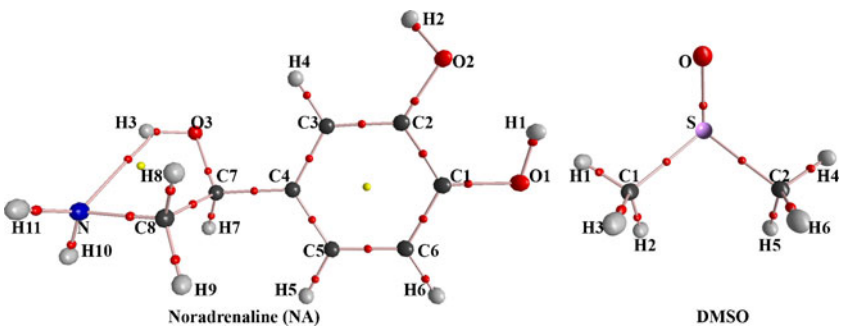

Fig. 1 Molecular graphs of free noradrenaline (NA) and DMSO (B) monomers. Large circles correspond to attractors attributed to atomic positions: gray, H; blue, N; black, C; red, O; S; purple. Small circles are attributed to critical points: red, bond critical point; yellow, ring critical point

acceptor sites to form H-bonds, respectively. The main H-acceptors of NA are the three oxygen atoms of the hydroxyl groups, and the oxygen atom is the unique H-acceptor in DMSO moiety. Moreover, similar to adrenaline [16], the benzene ring can act as a H-acceptor to form a π-H-bond. The main H-donor sites of NA may occur on the two phenolic hydroxyls as well as the hydroxyl linked with α-carbon. Moreover, the amino (NH_2, N) group as well as the methenyls (C3H4 on the benzene ring and C7H7) as a H-donor can also form H-bond with DMSO in a few complexes. DMSO can offer the methyl as a H-donor to form weak H-bond. The benzene ring can also offer a proton to the oxygen atom of DMSO to form a π-H-bond.

Structures

According to QTAIM, the presence of a bond critical point (BCP) between two atoms is a universal indicator of bonded interactions and the electron density, ρ_b, at the critical point is related to the bond strength or bond order. Therefore, the existence of BCP and the topological properties of electron density ρ_b can be used to study the nature of a H-bond. Based on the QTAIM, both inter- and intramolecular H-bonds can be characterized by the BCP between a H-donor (X-H) and a H-acceptor (Y). The coexistence of several H-bonds maybe results in the formation of a ring structure characterized by a ring critical point (RCP). Of course, the benzene ring of NA moiety also can be characterized by a RCP which has no relationship with a H-bond. Moreover, the distance between the BCP of H-bond and corresponding RCP can also be used as a criterion to measure the structural stability of the H-bond. The union between these two critical points represents bond cleavage and consequent ring opening [43]. In addition, a cage structure formed consequently by many H-bonds is characterized by a cage critical point (CCP). As shown in Fig. 1, the intramolecular $O3H3^{A}\cdots N^{A}$ H-bonds characterized by a BCP between H3···N form a five-membered ring which is characterized by corresponding RCP. Moreover, the intramolecular H-bond is weak since the distance between the BCP and the RCP is very short. In addition, similar to adrenaline [16], no intramolecular H-bond between the two phenolic hydroxyls can be found in NA on the basis of QTAIM and NBO analyses although it seems to exist from a viewpoint of structure.

All optimized complexes were presented in Fig. 2, and the structural parameters of H-bonds were listed in Table 1. The vibrational frequency calculations show that all optimized complexes have no imaginary frequencies and are stable structures. As shown in Fig. 2, each of the complexes involves multiple intermolecular H-bonds. The intramolecular $O3H3^{A}\cdots N^{A}$ H-bond involved in free NA still exist in NA-DMSO complexes except in the **AB6** and **AB10** complexes. Beside the intramolecular $O3H3^{A}\cdots N^{A}$ H-bond, another intramolecular H-bond formed between the two phenolic hydroxyls can be found in the **AB1** and **AB2** complexes. It is noteworthy that the bonding manner of the **AB1** and **AB2** complexes are similar, and the differences lie on the orientation of DMSO moiety.

The dominant intermolecular H-bonds in all complexes are formed between hydroxyls of NA moiety and an O atom of DMSO, while H-bonds involving the methyl (DMSO) or methenyls (C3H4 and C7H7 of NA) as a H-donor are weak and minor. For most complexes, the two phenolic hydroxyls of NA moiety are arranged on one side only after the formation of H-bonds with DMSO, while they are opposites in both **AB3** and **AB4** since they form the bifurcated H-bonds with the oxygen atom of DMSO simultaneously. The bonding manner in **AB3** and in **AB4** is similar, and the main difference is whether DMSO is on the same side with the side-chain of NA moiety.

The bifurcated H-bonds are too familiar and can be found in most complexes except **AB9**. Most of the bifurcated H-bonds involve an O atom of either DMSO moiety or hydroxyl (O3), and few involve either an O atom of the phenolic hydroxyl (O1) or the N atom of the amino group of NA. In addition, on the basis of QTAIM shown in Fig. 2, some di-hydrogen bonds can also be found in **AB1**, **AB5**, **AB6** and **AB7**. Of course, these di-hydrogen bonds seem to be weak because of the longer bond lengths and will be further discussed later.

Another possible H-bond is a π H-bond, which cannot be directly identified, as shown in Fig. 2, since there is no better way to deal directly with a π bond by QTAIM. However, from a viewpoint of structure, when the methyl of DMSO moiety is above the benzene ring, it has a tendency to form a π H-bond between the methyl and the benzene ring. For example, the $C2H6^{B}\cdots C3^{A}$ H-bond in the **AB1** complex seems to be a π H-bond rather than an intermolecular H-bond. Similar things happened in **AB2**, **AB3** and **AB4**, in which the H-bonds involving the methyl of DMSO and one carbon atom of the benzene ring should be regarded as π H-bonds. Unfortunately, neither QTAIM nor NBO analyses can give direct evidences for a π H-bond.

Structural parameters of H-bonds can give preliminary information on the nature of H-bonds. It is well known that the H-bond formation is connected with the elongation of the proton donating X-H bond (except of the special case of so-called blue-shifting H-bonds) as well as the shortening of H···Y bond. The shorter H···Y bond or the longer X-H bond, the stronger the interaction, and vice versa. As shown in Table 1, most H-bonds have positive $\Delta R_{X\text{-}H}$ values and are red-shifting H-bonds, which will be further discussed later. Moreover, because of the larger $\Delta R_{X\text{-}H}$ and the shorter H···Y bonds, the H-bonds involving the hydroxyls

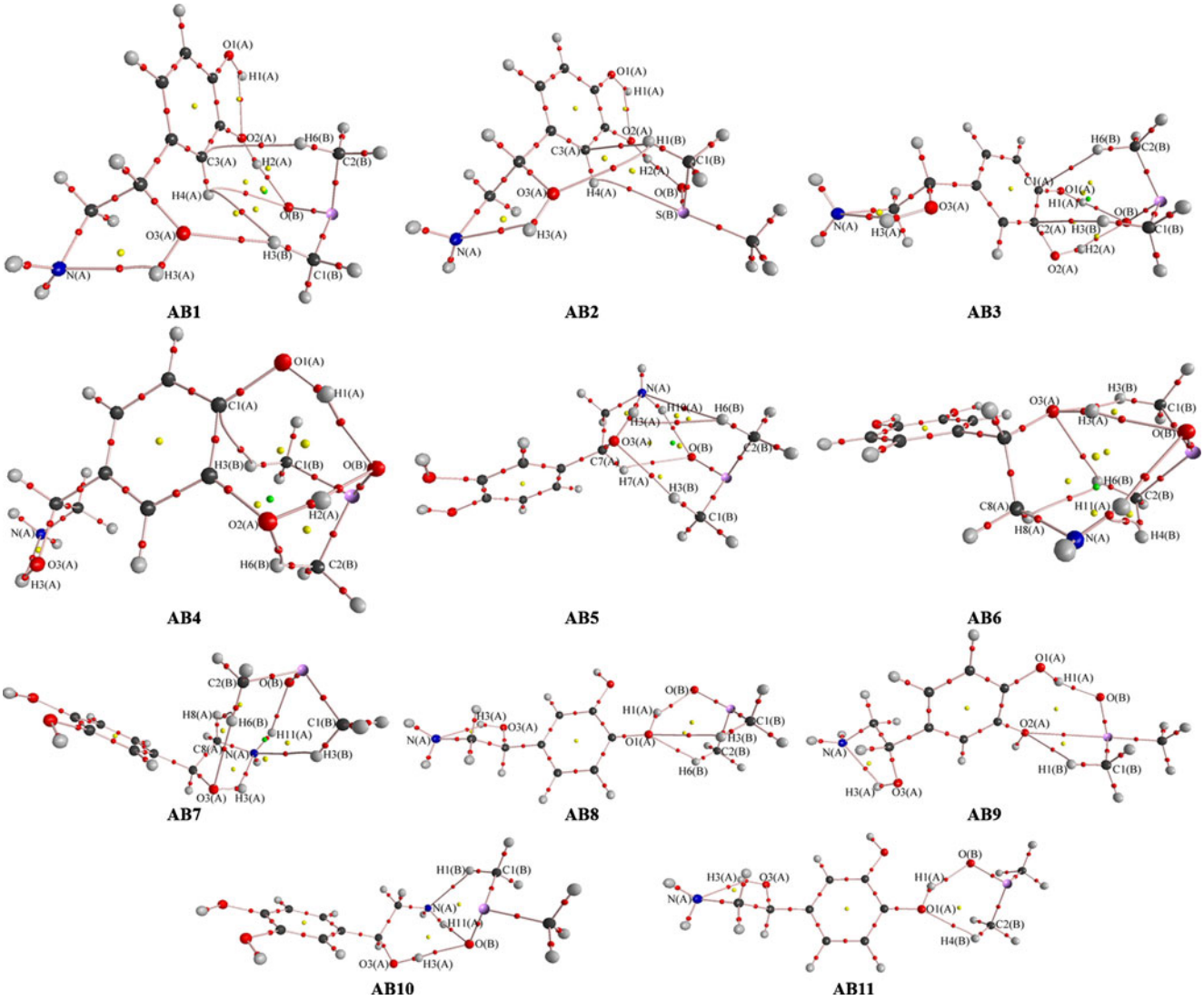

Fig. 2 Molecular graphs of NA-DMSO complexes. Large circles correspond to attractors attributed to atomic positions: gray, H; blue, N; black, C; red, O; S; purple. Small circles are attributed to critical points: red, bond critical point; yellow, ring critical point; green, cage critical point

of NA as H-donors are usually stronger than other H-bonds. Both the largest value (0.027 Å) of $\Delta R_{X\text{-}H}$ and the shortest H···Y bond (1.685 Å) are found in O2H2^{A}···O^{B} H-bond of **AB1**. This indicates that the O2H2^{A}···O^{B} H-bond in **AB1** is the strongest H-bond among NA-DMSO complexes. The O2H2^{A}···O^{B} H-bond in **AB2** involving the second shortest H···Y bond (1.717 Å) as well as the second largest value (0.024 Å) of $\Delta R_{X\text{-}H}$ should be the second strongest H-bond. Therefore, the phenolic hydroxyl O2H2 is the strongest H-donor among the three hydroxyls of NA, while the O3H3 hydroxyl is inclined to form the intramolecular H-bond with a N atom. In addition, other intermolecular H-bonds involving the hydroxyls or the amino as a H-donor are weaker than the above H-bonds and are stronger than those involving the methyl of DMSO or the methenyls (C3H4 and C7H7) of NA as H-acceptor.

The shorter H···Y bond, the stronger the interaction, and vice versa. However, because of different atoms as H-acceptors in different types of H-bonds, $R_{H\cdots Y}$ cannot be used directly for the comparison of H-bond strength. So a H-bond parameter, $\delta R_{H\cdots Y}$ [44], is defined as

$$\delta R_{H\cdots Y} = R_H^{vDW} + R_Y^{vDW} - R_{H\cdots Y}, \quad (1)$$

where R_H^{vDW} and R_Y^{vDW} are van der Waals radii of H and Y atoms given by Bondi [45], respectively, $R_{H\cdots Y}$ is the distance between a H-donor and a H-acceptor. As shown in Table 1, the maximum of $\delta R_{H\cdots Y}$ is 1.035 Å for the intermolecular O2H2^{A}···O^{B} H-bond in **AB1**, which seems to be the strongest H-bond. Of course, the intermolecular O2H2^{A}···O^{B} (1.003 Å) H-bond in **AB2** mentioned above is also a stronger H-bond due to the second largest $\delta R_{H\cdots Y}$. Moreover, due to the smaller $\Delta R_{X\text{-}H}$ and $\delta R_{H\cdots Y}$, the

Table 1 Structural parameters (bond lengths in Å, angles in degree) of H-bonds in NA-DMSO complexes calculated at ωB97XD/6-311++G(d,p) level

Complex	H-bond [a]	$R_{X\text{-}H}$	$R_{H\cdots Y}$	$\Delta R_{X\text{-}H}$ [b]	$\delta R_{H\cdots Y}$	∠X-H···Y
AB1	$O3H3^{A}\cdots N^{A}$	0.968	2.111	0.002	0.639	119.8
	$O1H1^{A}\cdots O2^{A}$	0.964	2.096	0.003	0.624	115.4
	$O2H2^{A}\cdots O^{B}$	0.985	1.685	0.027	1.035	167.2
	$C3H4^{A}\cdots O^{B}$	1.084	2.690	-0.001	0.030	113.0
	$C2H6^{B}\cdots C3^{A}$	1.091	2.667	0.000	0.233	138.8
	$C1H3^{B}\cdots O3^{A}$	1.093	2.257	0.001	0.463	162.0
	$C3H4^{A}\cdots H3C1^{B}$	1.084/1.093	2.456	-0.001/0.002	-0.056	111.6/126.5
AB2	$O3H3^{A}\cdots N^{A}$	0.967	2.130	0.001	0.620	119.3
	$O1H1^{A}\cdots O2^{A}$	0.965	2.099	0.003	0.621	115.6
	$O2H2^{A}\cdots O^{B}$	0.982	1.717	0.024	1.003	167.4
	$C3H4^{A}\cdots S^{B}$	1.084	2.839	-0.001	0.161	119.6
	$C1H1^{B}\cdots O3^{A}$	1.089	2.696	-0.001	0.024	118.1
	$C1H1^{B}\cdots C3^{A}$	1.089	2.654	-0.001	0.246	134.7
AB3	$O3H3^{A}\cdots N^{A}$	0.966	2.148	0.000	0.602	118.7
	$O1H1^{A}\cdots O^{B}$	0.972	1.809	0.010	0.911	159.2
	$O2H2^{A}\cdots O^{B}$	0.972	1.803	0.014	0.917	156.7
	$C2H6^{B}\cdots C1^{A}$	1.092	2.633	0.000	0.267	133.8
	$C1H3^{B}\cdots C2^{A}$	1.091	2.687	0.000	0.213	137.0
AB4	$O3H3^{A}\cdots N^{A}$	0.966	2.158	-0.001	0.592	118.1
	$O1H1^{A}\cdots O^{B}$	0.972	1.795	0.010	0.925	162.7
	$O2H2^{A}\cdots O^{B}$	0.971	1.841	0.013	0.879	153.7
	$C2H6^{B}\cdots O2^{A}$	1.091	2.541	0.000	0.179	126.2
	$C1H3^{B}\cdots C1^{A}$	1.092	2.651	0.000	0.249	128.2
AB5	$O3H3^{A}\cdots N^{A}$	0.971	2.009	0.005	0.741	123.3
	$NH10^{A}\cdots O^{B}$	1.020	2.019	0.007	0.701	152.8
	$C7H7^{A}\cdots O^{B}$	1.098	2.604	-0.004	0.116	128.5
	$C1H3^{B}\cdots O3^{A}$	1.093	2.304	0.002	0.416	159.3
	$C2H6^{B}\cdots N^{A}$	1.091	3.002	-0.001	-0.252	126.6
	$H3O3^{A}\cdots C2H6^{B}$	0.971/1.091	2.406	0.005/0.000	-0.006	118.2/153.3
AB6	$C2H4^{B}\cdots N^{A}$	1.091	2.974	0.001	-0.224	112.3
	$O3H3^{A}\cdots O^{B}$	0.973	1.839	0.007	0.881	156.5
	$NH11^{A}\cdots O^{B}$	1.017	2.070	0.006	0.650	166.8
	$C2H6^{B}\cdots O3^{A}$	1.091	2.612	0.000	0.108	128.7
	$C1H3^{B}\cdots O3^{A}$	1.092	2.610	0.000	0.110	132.3
	$C8H8^{A}\cdots H6C2^{B}$	1.097/1.091	2.392	0.003/0.000	0.008	119.0/119.5
AB7	$O3H3^{A}\cdots N^{A}$	0.973	1.988	0.007	0.762	123.4
	$NH11^{A}\cdots O^{B}$	1.018	2.015	0.007	0.705	146.7
	$C1H3^{B}\cdots N^{A}$	1.091	3.133	0.000	-0.383	129.6
	$C2H6^{B}\cdots O3^{A}$	1.092	2.384	0.001	0.336	173.5
	$C8H8^{A}\cdots H6C2^{B}$	1.092/1.092	2.450	-0.002/0.001	-0.050	110.9/104.4
AB8	$O3H3^{A}\cdots N^{A}$	0.966	2.148	0.000	0.602	118.6
	$O1H1^{A}\cdots O^{B}$	0.983	1.807	0.021	0.913	146.1
	$C2H6^{B}\cdots O1^{A}$	1.091	2.466	0.000	0.254	130.5
	$C1H3^{B}\cdots O1^{A}$	1.091	2.440	0.000	0.280	130.8
AB9	$O3H3^{A}\cdots N^{A}$	0.966	2.149	0.000	0.601	118.6
	$O1H1^{A}\cdots O^{B}$	0.980	1.764	0.018	0.956	159.9
	$C1H1^{B}\cdots O2^{A}$	1.089	2.493	-0.001	0.227	125.1
AB10	$O3H3^{A}\cdots O^{B}$	0.970	1.847	0.004	0.873	174.4

Table 1 (continued)

Complex	H-bond [a]	R_{X-H}	$R_{H\cdots Y}$	ΔR_{X-H} [b]	$\delta R_{H\cdots Y}$	∠X-H···Y
	$NH11^{A}\cdots O^{B}$	1.016	2.137	0.005	0.583	139.1
	$C1H1^{B}\cdots N^{A}$	1.092	2.481	0.003	0.269	135.0
AB11	$O3H3^{A}\cdots N^{A}$	0.966	2.140	0.000	0.610	118.9
	$O1H1^{A}\cdots O^{B}$	0.978	1.847	0.016	0.873	145.9
	$C2H4^{B}\cdots O1^{A}$	1.090	2.492	0.000	0.228	125.4

[a] Superscript "A" denote noradrenaline and "B" denote DMSO

[b] $\Delta R_{X-H} = R_{X-H}$ (complexes) - R_{X-H}(free monomer)

H-bonds formed between O/N atoms of DMSO/NA and methyl (DMSO) or methenyls (C3H4 and C7H7 of NA) as H-acceptor are weaker than those involving hydroxyls as a H-donor. In addition, the negative values of $\delta R_{H\cdots Y}$ can be found in the H-bonds formed between methyl (DMSO) and N atom (NA) in **AB5**, **AB6** and **AB7**, which means the H···N bond length is longer than the sum of the van der Waals radii of hydrogen and nitrogen atoms. Therefore, there are probably no interactions rather than hydrogen bonding interactions. Similarly, the di-hydrogen bonds in some complexes (**AB1**, **AB5**, **AB6** and **AB7**) are very weak because the H···H bond length is almost equal to the sum of the van der Waals radii of two hydrogen atoms. Therefore, according to the criteria of QTAIM, weak H-bonds might not qualify as true h-bonds; if the interest is to determine weak hydrogen bonds, other methods might be more amenable.

As shown in Table 1, for the intramolecular $O3H3^{A}\cdots N^{A}$ H-bond in **AB7**, the $R_{N1\text{-}H1}$ bond length is elongated and $\delta R_{H\cdots Y}$ is larger than that of free NA, which indicates that the strength of intramolecular $O3H3^{A}\cdots N^{A}$ H-bond is enhanced. The enhancement of the $O3H3^{A}\cdots N^{A}$ H-bond is attributed to the cooperative effect which exists among multiple H-bonds in complexes. Cooperativity, that is, the enhancement of the first H-bond between a proton donor and a proton acceptor when a second H-bond is formed between one of these two species and a third partner, is one of the hallmarks of hydrogen bonding [46–48]. When the intermolecular $NH11^{A}\cdots O^{B}$ and $C2H6^{B}\cdots O3^{A}$ H-bonds formed in **AB7**, the strong cooperative effect happened which further strengthen the intramolecular $O3H3^{A}\cdots N^{A}$ H-bond. A similar cooperative effect also occurs in other complexes (**AB1**, **AB2** and **AB5**), in which the intramolecular $O3H3^{A}\cdots N^{A}$ H-bond is enhanced because of the formation of new intermolecular H-bonds.

Vibrational frequency

The harmonic vibrational frequencies of H-bonds in NA-DMSO complexes and monomers as well as their shifts calculated at the ωB97XD/6-311++G(d,p) level were listed in Table 2. The red-shifts in the X-H stretching vibrational frequency have been traditionally considered one of the main fingerprints of H-bonds, assuming that formation of a H-bond weakens an X-H single bond. However, because of the concurrence of several inter- and intramolecular H-bonds in NA-DMSO complexes, it is not easy to calculate the shifts of X-H stretching vibrational modes if it mixes with other vibrational modes.

As shown in Table 2, the strong mixture among the two CH_3 stretching vibrational modes can be found in free DMSO molecules. Due to the strong mixture, multiple shift values are given for each CH_3 stretching vibration modes of DMSO moiety in the complex. Similar things also happened in NA-DMSO complexes. For example, the strong mixture among the two CH_3 stretching vibrational modes in both **AB8** results in the four shift values for the H-bonds involving methyl as H-donor, of course, these shifts are very small, which indicates that these H-bonds involving methyl as a H-donor are weak. The strong mixture among the bifurcated H-bond formed between O and the two phenolic hydroxyls in both **AB3** and **AB4**. Due to the strong mixture, four shift values of about -180∼-300 cm^{-1} are given for each phenolic hydroxyl stretching vibration modes of NA moiety in these complexes, which indicates that the bifurcated H-bond is the stronger red-shift one. The maximum shift of -521.7 cm^{-1} can be found in the $O2H2^{A}\cdots O^{B}$ H-bond of **AB1**, and the $O2H2^{A}\cdots O^{B}$ H-bond in **AB2** with a shift of -456.4 cm^{-1} is the second maximum of shift, so the two H-bonds are the strongest red-shift ones. This is consistent with the above discussion. Moreover, the shifts of H-bonds involving hydroxyls (NA) and an O atom (DMSO) are beyond one hundred wavenumbers and are dominant H-bonds, while other H-bonds with small shift usually are weaker. Especially, the H-bonds involving methyls of DMSO as H-donor have small positive shift values, which indicates that these H-bonds should be weak blue-shift ones. In addition, the intramolecular $O3H3^{A}\cdots N^{A}$ H-bond involves the shifts of about -30∼-130 cm^{-1} in the complexes (**AB1**, **AB2**, **AB5** and **AB7**), which indicates that the strengthening of the intramolecular $O3H3^{A}\cdots N^{A}$ H-bond among these complexes is attributed to the coopera-

Table 2 The X-H stretching vibrational frequencies (in cm^{-1}) of H-bonds in both NA-DMSO complexes and monomers

Complex	H-bond	$\nu_{H\text{-}X}$[a]	$\Delta\nu$
AB1	O3H3^{A}···N^{A}	3752.2(159)	-30.8
	O1H1^{A}···O2^{A}	3835.7(100)	-35.9
	O2H2^{A}···O^{B}	3408.8(1117)	-521.7
	C3H4^{A}···O^{B}	3212.1(2)[b]	7.8
	C2H6^{B}···C3^{A}	3176.4(3, a), 3168.5(1, a), 3060.9(10, s)	-0.1, 2.35, 1.5
	C1H3^{B}···O3^{A}	3171.9(6, a), 3155.0(14, a), 3048.4(26, s)	-4.6, -11.15, -11
AB2	O3H3^{A}···N^{A}	3756.6(149)	-26.4
	O1H1^{A}···O2^{A}	3822.7(104)	-48.9
	O2H2^{A}···O^{B}	3474.1(1213)	-456.4
	C3H4^{A}···S^{B}	3211.2(6)	6.9
	C1H1^{B}···O3^{A}	3193.7(4, a), 3066.1(16, s)[c], 3064.9(1, s)[c]	17.2, 6, 6.2
	C1H1^{B}···C3^{A}	3193.7(4, a), 3066.1(16, s)[c], 3064.9(1, s)[c]	17.2, 6, 6.2
AB3	O3H3^{A}···N^{A}	3786.7(128)	3.7
	O1H1^{A}···O^{B}+O2H2^{A}···O^{B}	3674.7(1094)[d], 3623.7(35)[d]	-196.9, -247.9, -255.8, -306.8
	C2H6^{B}···C1^{A}	3179.6(1, a), 3167.0(1, a)[c], 3059.9(8, s)	3.1, 0.85, 0.5
	C1H3^{B}···C2^{A}	3185.6(2, a), 3173.2(2, a)[c], 3066.2(10, s)	9.1, 7.05, 6.8
AB4	O3H3^{A}···N^{A}	3796.5(125)	13.5
	O1H1^{A}···O^{B}+O2H2^{A}···O^{B}	3689.3(983, a)[d], 3634.0(92, s)[d]	-182.3, -237.6, -241.2, -296.5
	C2H6^{B}···O2^{A}	3181.0(2, a), 3174.7(1, a)[c], 3065.0(10, s)	4.5, 8.55, 5.6
	C1H3^{B}···C1^{A}	3177.8(1, a), 3167.3(1, a)[c], 3059(6, s)	1.3, 1.15, -0.4
AB5	O3H3^{A}···N^{A}	3685.7(170)	-97.3
	NH10^{A}···O^{B}	3630.9(26, a), 3474.8(147, s)	-16.7, -85.2
	C7H7^{A}···O^{B}	3027.9(18)[e], 3024.1(39)[e]	53.5, 49.7
	C1H3^{B}···O3^{A}	3178.0(1, a), 3174.8(4, a)[c], 3065.8(8, s)	1.5, 8.65, 6.4
	C2H6^{B}···N^{A}	3152.5(7, a), 3042.7(26, s)	-24, -16.7
AB6	O3H3^{A}···O^{B}	3631.7(643)[f]	-151.3
	NH11^{A}···O^{B}	3614.2(30, a)[f],3520.1(54, s)[f]	-33.4, -39.9
	C2H4^{B}···N^{A}	3175.3(1, a)[c], 3168.0(1, a)[c], 3059.7(5, s)[c]	-1.2, 1.85, 0.3
	C2H6^{B}···O3^{A}	3175.3(1, a)[c], 3168.0(1, a)[c], 3059.7(5, s)[c]	-1.2, 1.85, 0.3
	C1H3^{B}···O3^{A}	3178.6(1, a)[c], 3170.9(1, a)[c], 3061.7(10, s)[c]	2.1, 4.75, 2.3
AB7	O3H3^{A}···N^{A}	3654.9(184)	-128.1
	NH11^{A}···O^{B}	3635.0(36, a), 3498.3(158, s)	-12.6, -61.7
	C1H3^{B}···N^{A}	3180.5(1, a)[c], 3172.5(3, a)[c], 3064.3(6, s)	4, 6.35, 4.9
	C2H6^{B}···O3^{A}	3169.7(6, a)[c], 3159.7(6, a)[c], 3050.3(17, s)[c]	-6.8, -6.45, -9.1
AB8	O3H3^{A}···N^{A}	3781.2(136)	-1.8
	O1H1^{A}···O^{B}	3476.2(1001)	-395.4
	C2H6^{B}···O1^{A}+C1H3^{B}···O1^{A}	3177.9(3, a)[g], 3174.8(1, a)[g], 3167.0(2, a)[g], 3163.9(1, a)[g], 3057.6(21, s)[g], 3055.8(7, s)[g]	0.9, -1.2, -0.8, -0.6, -2.5, -2.9
AB9	O3H3^{A}···N^{A}	3784.9(135)	1.9
	O1H1^{A}···O^{B}	3509.0(1424)	-362.6
	C1H1^{B}···O2^{A}	3186.8(1, a), 3059.6(13, s)[c]	10.3, 0.2
AB10	O3H3^{A}···O^{B}	3680.8(849)	-102.2
	NH11^{A}···O^{B}	3617.5(11, a), 3526.8(22, s)	-30.1, -33.2
	C1H1^{B}···N^{A}	3153.6(11, a), 3048.3(22, s)	-22.9, -11.1
AB11	O3H3^{A}···N^{A}	3782.5(136)	-0.5
	O1H1^{A}···O^{B}	3576.6(997)	-295
	C2H4^{B}···O1^{A}	3181.9(3), 3059.2(7)[c]	5.4, -0.2
NA	O1-H1	3871.6(114)	
	O2-H2	3930.5(88)	

Table 2 (continued)

Complex	H-bond	$\nu_{H\text{-}X}$[a]	$\Delta\nu$
	O3-H3	3783.0(136)	
	H10-N-H11	3647.6(8, a), 3560.0(2, s)	
	C3-H4	3204.3(5)	
	C7-H7	2974.4(50)	
DMSO	CH_3	3177.0(3, a)[g], 3176.0(1, a)[g], 3167.8(10, a)[g], 3164.5(0, a)[g], 3060.1(8, s)[g], 3058.7(5, s)[g]	

[a] "s" denote symmetric stretching vibrational modes, and "a" denote asymmetric stretching vibrational modes. Numbers in parentheses are intensity (in km·mol^{-1}) of vibrational modes

[b] mixed with other vibrational modes slightly

[c] mixed with symmetric CH_3 stretching vibrational modes slightly

[d] strong mixture between the O-H stretching vibrational modes

[e] The O-H stretching vibrational mode mixes with the asymmetric CH_2 stretching vibrational mode strongly

[f] The O-H stretching vibrational mode mixes with the NH_2 stretching vibrational modes

[g] strong mixture between the two CH_3 stretching vibrational modes

tive effect. Moreover, the strongest cooperative effect in AB7 is confirmed by the largest shift value of -128.1 cm^{-1} of the intramolecular O3H3^{A}···N^{A} H-bond. On the contrary, no obvious evidence for the cooperativity of a H-bond in other complexes can be found since the shifts of the intramolecular O3H3^{A}···N^{A} H-bond are very small or positive.

QTAIM analysis

The QTAIM analysis has been carried out to deepen the nature of the H-bond interactions, and the results are listed in Table 3. According to QTAIM, both electron density (ρ_b) and its Laplacian ($\nabla^2\rho_b$) at the BCP of XH···Y H-bond are good measures of the strength of H-bond. According to the criteria of H-bonds proposed by Popelier, all H-bonds of the studied complexes have positive $\nabla^2\rho_b$ values and fall within the 0.02 ~ 0.15 a.u. range, while ρ_b must fall between 0.002 and 0.04 a.u. [31]. As shown in Table 3, for the O2H2^{A}···O^{B} H-bond in **AB1**, the ρ_b (0.04405) of is beyond the upper-limit of the range, the $\nabla^2\rho_b$ (0.14542) is the maximum value among all H-bonds and is close to the upper-limit of the range. Therefore, the O2H2^{A}···O^{B} H-bond in **AB1** is the strongest H-bond and a partial covalent character is attributed to the H-bond, which is consistent with the above discussion from the viewpoint of structure. Similarly, the O2H2^{A}···O^{B} H-bond in **AB2** is a strong H-bond as well because the ρ_b (0.0397) and $\nabla^2\rho_b$ (0.13883) are very close to the upper-limit of the ranges, respectively. As shown in Table 3, it can be found that most intermolecular H-bonds formed between hydroxyls of NA and an O atom of DMSO are strong ones, moreover, the H-bonds involving two phenolic hydroxyls of NA moiety usually are stronger than those involving the other hydroxyl. All ρ_b and $\nabla^2\rho_b$ values of other H-bonds fall within the ranges. Moreover, due to the smaller ρ_b and its Laplace values, the H-bonds formed between O/N atoms of DMSO/NA and methyl (DMSO) or methenyls (C3H4 and C7H7 of NA) as H-acceptor are weaker than those involving hydroxyls as H-donor. Especially, for the H-bonds formed between methyl (DMSO) and N atom (NA) in **AB5**, **AB6** and **AB7**, the $\nabla^2\rho_b$ is beyond the lower-limit range, and the H···N bond length is longer than the sum of the van der Waals radii of hydrogen and nitrogen atoms, thus there are probably no interactions between hydrogen and nitrogen atoms among these complexes. Therefore, QTAIM is not an exclusive criterion to confirm the existence of a very weak H-bond. Similarly, for the di-hydrogen bonds in some complexes (**AB1**, **AB5**, **AB6** and **AB7**), the ρ_b of them are close to the lower-limit of the range and the $\nabla^2\rho_b$ are beyond the lower-limit value, which indicates that these di-hydrogen bonds are very weak and a partial van der Waals interactions character is attributed to the H-bonds. In addition, the cooperativity of the H-bond in complexes can be learned from the results of QTAIM as well. As shown in Table 3, the values of ρ_b (0.03134) as well as $\nabla^2\rho_b$ (0.09940) of the intramolecular O3H3^{A}···N^{A} H-bond in **AB7** are the maximum among complexes and are larger than those of free NA, which indicates that the strong cooperative effect happened in **AB7** and is consistent with the above discussion. Similar cooperative effect can be found in other complexes (**AB1**, **AB2** and **AB5**) as well, in which the values of ρ_b as well as $\nabla^2\rho_b$ of the intramolecular O3H3^{A}···N^{A} H-bonds are larger than that of free NA.

Generally, the ρ_b decreases as a result of the elongation of the corresponding bond. The opposite occurs when the bond length shortens. Therefore, a relationship between ρ_b and H···Y bond length of X-H···Y H-bond is predictable.

Table 3 Electron density (ρ_b) and Laplacian of the electron density ($\nabla^2\rho_b$) in a.u. at BCPs of H-bonds in both NA-DMSO complexes and NA monomer obtained by QTAIM analysis

Complex	H-bond	ρ_b	$\nabla^2\rho_b$	Complex	H-bond	ρ_b	$\nabla^2\rho_b$
AB1	O3H3^{A}···N^{A}	0.02406	0.08535	**AB6**	C2H4^{B}···N^{A}	0.00474	0.01860
	O1H1^{A}···O2^{A}	0.02057	0.09393		O3H3^{A}···O^{B}	0.03302	0.11444
	O2H2^{A}···O^{B}	0.04405	0.14542		NH11^{A}···O^{B}	0.02033	0.07182
	C3H4^{A}···O^{B}	0.00832	0.02758		C2H6^{B}···O3^{A}	0.00847	0.02440
	C2H6^{B}···C3^{A}	0.00878	0.02456		C1H3^{B}···O3^{A}	0.00668	0.02303
	C1H3^{B}···O3^{A}	0.01372	0.04657		C8H8^{A}···H6C2^{B}	0.00575	0.01819
	C3H4^{A}···H3C1^{B}	0.00497	0.01669	**AB7**	O3H3^{A}···N^{A}	0.03134	0.09940
AB2	O3H3^{A}···N^{A}	0.02318	0.08327		NH11^{A}···O^{B}	0.02262	0.08303
	O1H1^{A}···O2^{A}	0.02070	0.09308		C1H3^{B}···N^{A}	0.00365	0.01094
	O2H2^{A}···O^{B}	0.03971	0.13883		C2H6^{B}···O3^{A}	0.01207	0.03366
	C3H4^{A}···S^{B}	0.00738	0.02694		C8H8^{A}···H6C2^{B}	0.00591	0.01956
	C1H1^{B}···O3^{A}	0.00647	0.02319	**AB8**	O3H3^{A}···N^{A}	0.02248	0.08174
	C1H1^{B}···C3^{A}	0.00818	0.02304		O1H1^{A}···O^{B}	0.03484	0.11961
AB3	O3H3^{A}···N^{A}	0.02251	0.08164		C2H6^{B}···O1^{A}	0.00922	0.03112
	O1H1^{A}···O^{B}	0.03424	0.12181		C1H3^{B}···O1^{A}	0.01029	0.03332
	O2H2^{A}···O^{B}	0.03533	0.12372	**AB9**	O3H3^{A}···N^{A}	0.02245	0.08162
	C2H6^{B}···C1^{A}	0.00857	0.02430		O1H1^{A}···O^{B}	0.03602	0.12772
	C1H3^{B}···C2^{A}	0.00737	0.02316		C1H1^{B}···O2^{A}	0.01011	0.03313
AB4	O3H3^{A}···N^{A}	0.02204	0.08097	**AB10**	O3H3^{A}···O^{B}	0.03020	0.11134
	O1H1^{A}···O^{B}	0.03480	0.12498		NH11^{A}···O^{B}	0.01871	0.06603
	O2H2^{A}···O^{B}	0.03303	0.11509		C1H1^{B}···N^{A}	0.01114	0.03280
	C2H6^{B}···O2^{A}	0.00906	0.02889	**AB11**	O3H3^{A}···N^{A}	0.02277	0.08256
	C1H3^{B}···C1^{A}	0.00899	0.02530		O1H1^{A}···O^{B}	0.03042	0.11252
AB5	O3H3^{A}···N^{A}	0.02914	0.09728		C2H4^{B}···O1^{A}	0.00904	0.03049
	NH10^{A}···O^{B}	0.02218	0.08097	NA	O3H3^{A}···N^{A}	0.02266	0.08212
	C7H7^{A}···O^{B}	0.00880	0.02598				
	C1H3^{B}···O3^{A}	0.01365	0.04159				
	C2H6^{B}···N^{A}	0.00469	0.01392				
	C2H6^{B}···H3O3^{A}	0.00425	0.01505				

Because of different atoms as H-acceptor in different H-bonds, the H-bond parameter $\delta R_{H\cdots Y}$ defined in Eq. 1 is used to replace H···Y bond length to carry out correlation analysis. As shown in Fig. 3, a good linear relationship between $\ln\rho_b$ and $\delta R_{H\cdots Y}$ was found and the fitted equation can be expressed as

$$\ln\rho_b = -5.0767 + 1.8964\delta R_{H\cdots Y} \quad r = 0.9849 \qquad (2)$$

where r is the correlation coefficient. Therefore, the estimate results of the strength of H-bonds by QTAIM are consistent with those by structural analysis.

NBO analysis and energy

The NBO analysis was also performed here to deepen the nature of H-bonds and the result was listed in Table 4. According to NBO theory [33], the second-perturbation energies $E(2)$ lowering is responsible for the orbital interaction of H-bond, the larger $E(2)$ values correspond to a stronger charge-transfer (CT) effect that happened in the H-bond. As shown in Table 4, the O atom involved in most of intermolecular H-bonds has different branches: one has sp hybrid characteristics, and the others have more p hybrid characteristics; they corresponds to different $E(2)$ values, respectively. On the contrary, the O atom involved in intramolecular H-bond is mainly of p character. In addition, the N atom involved in the H-bond is mainly of p character as well. The largest $E(2)$ value of 27.30 kcal·mol^{-1} is found for the O2H2^{A}···O^{B} H-bond in **AB1**, which indicates the strongest CT effect happened in **AB1**. Similarly, a stronger CT effect happened in O2H2^{A}···O^{B} (**AB2**) and O1H1^{A}···O^{B} (**AB9**) H-bonds because of the larger $E(2)$ values. Moreover, the CT effect happened in the

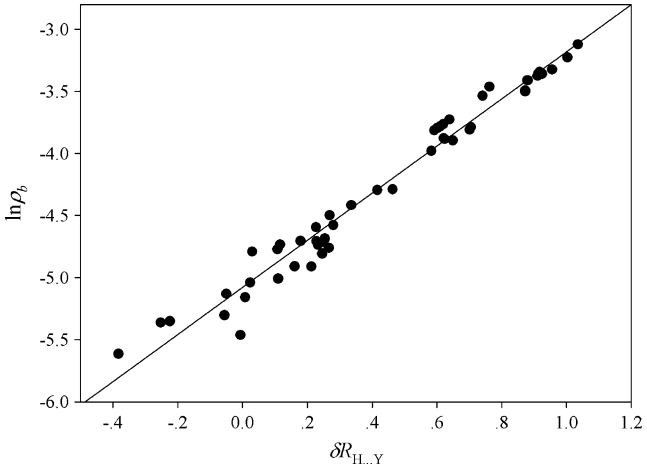

Fig. 3 Correlation between the electron density (ρ_b) at BCPs and $\delta R_{H\cdots Y}$ in H-bonds

H-bonds involving hydroxyls as H-donors are stronger than those that happened in other H-bonds. However, no information of CT effect on the H-bonds formed between methyl (DMSO) and a N atom (NA) in **AB5**, **AB6** and **AB7** were given by NBO analyses, which indicates that no CT effect happened in these H-bonds, that is, there are probably no interactions between hydrogen and nitrogen atoms among these complexes, which is consistent with the above discussion. Similarly, NBO analysis cannot give information of CT effect on the di-hydrogen bonds in some complexes (**AB1**, **AB5**, **AB6** and **AB7**) as well, which attribute to van der Waals interactions character to a great extent. In addition, the results of NBO can also give evidence for the cooperativity of a H-bond in complexes. As shown in Table 4, the strong cooperative effect in **AB7** is confirmed by the largest $E(2)$ value of 10.99 kcal·mol^{-1} of the intramolecular O3H3$^{A}\cdots$N^{A} H-bond, which also agree with the above discussion. A similar cooperative effect can be found in other complexes (**AB1**, **AB2** and **AB5**) as well, in which the values of $E(2)$ of the intramolecular O3H3$^{A}\cdots$N^{A} H-bonds are larger than that of free NA.

Beside the QTAIM and NBO method, other methods were applied to deepen the nature of H-bonds. Despite the vast literature on the bonding mechanism of H-bonds there was no unified explanation for all red- and blue-shift H-bonds. It is noteworthy that Politzer et al. interpreted blue shifting and red shifting in terms of the Hermannson equation [49] and σ-holes [50–56] successfully. Especially, according to the research of Politzer et al., the molecular surface electrostatic potential of

Table 4 The second-perturbation energies $E(2)$ (in kcal·mol^{-1}) of H-Bonds in both NA-DMSO complexes and NA monomer obtained by NBO analysis

Complex	H-bond	$E(2)$ [a]	Complex	H-bond	$E(2)$ [a]
AB1	O3H3$^{A}\cdots$N^{A}	5.65	**AB6**	C2H4$^{B}\cdots$N^{A}	0.16
	O1H1$^{A}\cdots$O2^{A}	1.81		O3H3$^{A}\cdots$O^{B}	4.68 (11.05)
	O2H2$^{A}\cdots$O^{B}	11.70 (2.88, 12.72)		NH11$^{A}\cdots$O^{B}	1.85 (0.25, 4.89)
	C3H4$^{A}\cdots$O^{B}	0.11 (0.26)		C2H6$^{B}\cdots$O3^{A}	0.11 (0.82)
	C1H3$^{B}\cdots$O3^{A}	3.04 (0.89)		C1H3$^{B}\cdots$O3^{A}	0.46 (0.09)
AB2	O3H3$^{A}\cdots$N^{A}	5.09	**AB7**	O3H3$^{A}\cdots$N^{A}	10.99
	O1H1$^{A}\cdots$O2^{A}	1.81		NH11$^{A}\cdots$O^{B}	3.05 (3.26, 0.36)
	O2H2$^{A}\cdots$O^{B}	8.73 (4.92, 10.61)		C1H3$^{B}\cdots$N^{A}	0.19
	C1H1$^{B}\cdots$O3^{A}	0.18		C2H6$^{B}\cdots$O3^{A}	0.38 (2.91)
AB3	O3H3$^{A}\cdots$N^{A}	4.66	**AB8**	O3H3$^{A}\cdots$N^{A}	4.66
	O1H1$^{A}\cdots$O^{B}	5.66 (5.37, 5.48)		O1H1$^{A}\cdots$O^{B}	6.18 (11.83)
	O2H2$^{A}\cdots$O^{B}	5.47 (7.45, 4.30)		C2H6$^{B}\cdots$O1^{A}	0.84 (0.22)
AB4	O3H3$^{A}\cdots$N^{A}	4.38		C1H3$^{B}\cdots$O1^{A}	0.76 (0.54)
	O1H1$^{A}\cdots$O^{B}	6.30 (3.44, 7.54)	**AB9**	O3H3$^{A}\cdots$N^{A}	4.66
	O2H2$^{A}\cdots$O^{B}	4.46 (8.68, 1.91)		O1H1$^{A}\cdots$O^{B}	6.76 (0.95, 13.46)
	C2H6$^{B}\cdots$O2^{A}	0.12 (0.39)		C1H1$^{B}\cdots$O2^{A}	0.10 (0.49)
AB5	O3H3$^{A}\cdots$N^{A}	8.93	**AB10**	O3H3$^{A}\cdots$O^{B}	3.66 (10.86, 1.30)
	NH10$^{A}\cdots$O^{B}	3.19 (2.23, 1.75)		NH11$^{A}\cdots$O^{B}	1.07 (3.03)
	C7H7$^{A}\cdots$O^{B}	0.38 (0.21, 0.40)		C1H1$^{B}\cdots$N^{A}	2.09
	C1H3$^{B}\cdots$O3^{A}	0.65 (3.00)	**AB11**	O3H3$^{A}\cdots$N^{A}	4.81
	C2H6$^{B}\cdots$N^{A}	0.3		O1H1$^{A}\cdots$O^{B}	4.82 (0.39, 9.25)
NA	O3H3$^{A}\cdots$N^{A}	4.77		C2H4$^{B}\cdots$O1^{A}	0.70 (0.11)

[a] The values are O sp hybrid branch to form the H-bond; those in the parentheses are O p hybrid branch. The lone pair of N atom is mainly of p character. See discussion in the text

DMSO reveals positive σ-holes on the sulfur on the extension of the O-S bond [57]. The resulting arrays of positive and negative site in DMSO makes possible a variety of simultaneous intermolecular hydrogen bonding interactions. Therefore, the H-bonds among NA-DMSO complexes can be interpreted in terms of σ-hole interactions, which will be discussed in detail in our future research.

According to NBO theory [33], the actual interaction energy (ΔE_{int}) is decomposed into the charge-transfer (CT) and non-charge-transfer (NCT) parts

$$\Delta E_{int} = \Delta E_{NCT} + \Delta E_{CT} \quad (3)$$

where ΔE_{CT} account for the orbital interaction and polarization interactions, ΔE_{NCT} consists of the classical electrostatic interaction and the Pauli steric repulsion interaction. The ΔE_{CT} term (always negative) were obtained by summarizing $E(2)$ for intermolecular H-bonds in Table 4, and the ΔE_{NCT} term can be obtained from Eq. 3. Furthermore, the binding energy (ΔE) of NA-DMSO complex is influenced by the deformations of monomers and is decomposed as

$$\Delta E = \Delta E_{prep} + \Delta E_{int}, \quad (4)$$

where the preparation energy (ΔE_{prep}) is the amount of energy required to deform the separate bases from their free monomer structure to the geometry that they acquire in the pair complex; ΔE_{int} represents the actual energy change when the prepared bases are combined to form the pair complex. Namely,

$$\Delta E_{prep} = E_{NA-DMSO} - E_{DMSO(NA)} - E_{NA(DMSO)} \quad (5)$$

$$\Delta E_{int} = E_{NA-DMSO} - E_{DMSO} - E_{NA}, \quad (6)$$

where $E_{NA\text{-}DMSO}$ is the energy of NA-DMSO complex, $E_{DMSO(NA)}$ (or $E_{NA(DMSO)}$) is the energy of DMSO (or NA) monomer when all the nucleus structure units of NA (or DMSO) are considered as puppet atoms of carrying an empty orbital; E_{DMSO} (or E_{NA}) is the energy of the most stable DMSO (or NA) molecule.

The ΔE of NA-DMSO complexes were decomposed into several terms summarized in Table 5. For most complexes, the two phenolic hydroxyls of NA moiety are arranged on one side only after the formation of H-bonds with DMSO, while they are opposites in both **AB3** and **AB4** since they form the bifurcated H-bonds with the oxygen atom of DMSO simultaneously. Therefore, both **AB3** and **AB4** are predicted to have serious deformation, which can be learned from the two largest ΔE_{prep} values (9.29 and 9.11 kcal·mol^{-1}, respectively) of them. The clearage of intramolecular O3H3^{A}···N^{A} H-bond in **AB6** and **AB10** leads to serious deformations, which are responsible for the larger ΔE_{prep} values (5.58 and 6.48 kcal·mol^{-1}, respectively). The serious deformations in these complexes (**AB3**, **AB4**, **AB6** and **AB10**) counteract the strong hydrogen bonding interaction to a great extent. Therefore, the binding energies (ΔE) of them are smaller than those of others. The intramolecular O3H3^{A}···N^{A} H-bonds still exist in other complexes, which are predicted to have small deformation. By and large, the order of ΔE_{int} is consistent with ΔE except those complexes (**AB3**, **AB4**, **AB6** and **AB10**) with serious deformations. The smallest ΔE_{prep} (0.85 kcal·mol^{-1}) of **AB11** does not mean that it is the most stable complex because of the weaker hydrogen bonding interactions. **AB1** is the most stable complex which involves the strongest O2H2^{A}···O^{B} H-bond, more importantly, its deformation is small. Therefore, both hydrogen bonding interaction and structural deformation can affect the stability of NA-DMSO complexes. In addition, as shown in Table 5, for most NA-DMSO complexes, the absolute values of ΔE_{CT} is larger than ΔE_{NCT}, because the hydrogen bonding interaction is a

Table 5 Total energy (E), preparation energies (ΔE_{prep}), charge-transfer energies (ΔE_{CT}), non-charge-transfer energies (ΔE_{NCT}), interaction energies (ΔE_{int}), and binding energies (ΔE) of the NA-DMSO complexes calculated at ωB97XD/6-311++G(d,p) level[a]

Complex	E	ΔE_{int}	ΔE_{prep}	ΔE_{CT}	ΔE_{NCT}	ΔE
AB1	-1144.822973	-15.88	1.86	-31.60	15.72	-14.02
AB2	-1144.81964	-13.79	2.19	-24.44	10.65	-11.60
AB3	-1144.818747	-13.23	9.29	-33.73	20.50	-3.94
AB4	-1144.816317	-11.70	9.11	-32.84	21.14	-2.59
AB5	-1144.812242	-9.14	0.95	-12.11	2.97	-8.19
AB6	-1144.811427	-8.63	5.58	-24.20	15.57	-3.05
AB7	-1144.810428	-8.01	1.78	-10.15	2.14	-6.23
AB8	-1144.81014	-7.82	1.03	-20.37	12.55	-6.79
AB9	-1144.809595	-7.48	1.87	-21.76	14.28	-5.61
AB10	-1144.808923	-7.06	6.48	-22.01	14.95	-0.58
AB11	-1144.807755	-6.33	0.85	-15.27	8.94	-5.48
NA	-591.684966					
DMSO	-553.112704					

[a] The total energy of complexes involve ZPVE and BSSE correction, while the energy of the monomers (NA and DMSO) involve ZPVE correction. All energies are in kcal·mol^{-1} except the total energy (in Hartree)

short-distance force, while the electrostatic interaction is a long-distance force; namely, the former should be predominant as two monomers get together.

Conclusions

The complexes formed between NA and DMSO have been investigated at ωB97XD/ 6-311++G(d,p) level. The nature of H-bonds has been analyzed through structures, energies, frequencies and electron density topological analysis. Multiple H-bonds including intra- and intermolecular H-bonds are formed in complexes. The H-bonds involving hydroxyls (NA) and O atoms (DMSO) are dominant intermolecular H-bonds and are stronger than other H-bonds involving methyl of DMSO as H-donor. The weak H-bonds also include π H-bonds which involve the benzene ring as a H-donor or a H-acceptor. Especially, the QTAIM results identified the weak H-bonds formed between methyl (DMSO) and N atom (NA) in some complexes (**AB5**, **AB6** and **AB7**), which cannot be further confirmed by NBO and other methods, so there are probably no interactions between hydrogen and nitrogen atoms among these complexes. The intramolecular $O3H3^{A}\cdots N^{A}$ H-bond in some complexes were strengthened by the formations of new intermolecular H-bonds, which attribute to the cooperativity of H-bonds in complexes and can be learned from the results of structures, NBO and QTAIM analyses. The results show that the stability of NA-DMSO complexes is influenced by hydrogen bonding interactions and structural deformations. **AB1** with smaller deformation is the most stable complex, in which the $O2H2^{A}\cdots O^{B}$ H-bond is the strongest H-bond as well, while both serious deformation (such as **AB3**, **AB4**, **AB6** and **AB10**) and weaker hydrogen bonding interaction (such as **AB11**) will weaken the stability of the complex. In addition, the electron density (ρ_b) at BCPs significantly correlates with the H-bond parameter $\delta R_{H\cdots Y}$. This study provides the geometrical, energetical, and topological information of hydrogen bonding interactions in the NA-DMSO complexes and helps to elucidate the electrochemical behavior, pharmacology, pharmacodynamics of NA in DMSO.

Acknowledgments This work is supported by Tianjin Science and Technology Development Fund Projects in Colleges and Universities (No. 20080504).

References

1. Song YZ (2007) Theoretical study on the electrochemical behavior of norepinephrine at Nafion multi-walled carbon nanotubes modified pyrolytic graphite electrode. Spectrochim Acta Pt A Mol Biomol Spectrosc 67:1169–1177
2. Baron R, Zayats M, Willner I (2005) Dopamine-, L-DOPA-, adrenaline-, and noradrenaline- induced growth of Au nanoparticles: assays for the detection of neurotransmitters and of tyrosinase activity. Anal Chem 77:1566–1571
3. Chen SM, Peng KT (2003) The electrochemical properties of dopamine, epinephrine, norepinephrine, and their electrocatalytic reactions on cobalt(II) hexacyanoferrate films. J Electroanal Chem 547:179–189
4. Perati PR, Cheng J, Jandik P, Hanko VP (2010) Disposable carbon electrodes for liquid chromatographic detection of catecholamines in blood plasma samples. Electroanalysis 22:325–332
5. Chen W, Lin XH, Luo HB, Huang LY (2005) Electrocatalytic oxidation and determination of norepinephrine at poly(cresol red) modified glassy carbon electrode. Electroanalysis 17:941–945
6. Dong H, Wang SH, Liu AH, Galligan JJ, Swain GM (2009) Drug effects on the electrochemical detection of norepinephrine with carbon fiber and diamond microelectrodes. J Electroanal Chem 632:20–29
7. Luczak T (2009) Electroanalysis of norepinephrine at bare gold electrode pure and modified with gold nanoparticles and s-functionalized self-assembled layers in aqueous solution. Electroanalysis 12:1539–1549
8. Seol H, Jeong H, Jeon S (2009) A selective determination of norepinephrine on the glassy carbon electrode modified with poly (ethylenedioxypyrrole dicarboxylic acid) nanofibers. J Solid State Electrochem 13:1881–1887
9. Yao H, Li SG, Tang YH, Chen Y, Chen YZ, Lin XH (2009) Selective oxidation of serotonin and norepinephrine over eriochrome cyanine R film modified glassy carbon electrode. Electrochim Acta 54:4607–4612
10. Alagona G, Ghio C (2002) Interplay of intra- and intermolecular H-bonds for the addition of a water molecule to the neutral and N-protonated forms of noradrenaline. Int J Quantum Chem 90:641–656
11. Nagy PI, Alagona G, Ghio C, Takacs-Novak K (2003) Theoretical conformational analysis for neurotransmitters in the gas phase and in aqueous solution. Norepinephrine. J Am Chem Soc 125:2770–2785
12. Snoek LC, van Mourik T, Carcabal P, Simons JP (2003) Neurotransmitters in the gas phase: hydrated noradrenaline. Phys Chem Chem Phys 5:4519–4526
13. Snoek LC, Van Mourik T, Simons JP (2003) Neurotransmitters in the gas phase: a computational and spectroscopic study of noradrenaline. Mol Phys 101:1239–1248
14. Macleod NA, Simons JP (2004) Beta-blocker conformations in the gas phase: 2-phenoxy ethylamine, its hydrated clusters and 3-phenoxy propanolamine. Phys Chem Chem Phys 6:2878–2884
15. Van Mourik T (2004) The shape of neurotransmitters in the gas phase: a theoretical study of adrenaline, pseudoadrenaline, and hydrated adrenaline. Phys Chem Chem Phys 6:2827–2837
16. Huang ZG, Dai YM, Yu L (2010) Density functional theory and topological analysis on the hydrogen bonding interactions in N-protonated adrenaline-DMSO complexes. Struct Chem 21:863–872
17. Yu ZY, Guo DJ, Wang HQ (2004) Theoretical study on the hydrogen bond interaction between adrenaline and dimethyl sulphoxide. Chin J Chem Phys 17:149–154
18. Huang ZG, Yu L, Dai YM (2010) Density functional theory and topological analysis on the hydrogen bonds in cysteine-propanoic acid complexes. Struct Chem 21:855–862
19. Huang ZG, Yu L, Dai YM (2010) Combined DFT with NBO and QTAIM studies on the hydrogen bonds in $(CH_3OH)_n$ (n=2-8) clusters. Struct Chem 21:565–572
20. Rappe AK, Bernstein ER (2000) Ab initio calculation of nonbonded interactions: are we there yet? J Phys Chem A 104:6117–6128

21. Grimme S (2004) Accurate description of van der Waals complexes by density functional theory including empirical corrections. J Comput Chem 25:1463–1473
22. Schwabe T, Grimme S (2007) Double-hybrid density functionals with long-range dispersion corrections: higher accuracy and extended applicability. Phys Chem Chem Phys 9:3397–3406
23. Zhao Y, Truhlar DG (2006) Comparative DFT study of van der Waals complexes: Rare-gas dimers, alkaline-earth dimers, zinc dimer, and zinc-rare-gas dimers. J Phys Chem A 110:5121–5129
24. Zhao Y, Truhlar DG (2008) The M06 suite of density functionals for main group thermochemistry, thermochemical kinetics, noncovalent interactions, excited states, and transition elements: two new functionals and systematic testing of four M06-class functionals and 12 other functionals. Theor Chem Acc 120:215–241
25. Chai JD, Head-Gordon M (2008) Long-range corrected hybrid density functionals with damped atom-atom dispersion corrections. Phys Chem Chem Phys 10:6615–6620
26. Johnson ER, Mackie ID, DiLabio GA (2009) Dispersion interactions in density-functional theory. J Phys Org Chem 22:1127–1135
27. Huang ZG, Yu L, Dai YM, Wang HK (2010) Hydrogen bonding interactions in cysteine-urea complexes: theoretical studies of structures, properties and topologies. J Mol Struct THEOCHEM 960:98–105
28. Rao L, Ke HW, Fu G, Xu X, Yan YJ (2009) Performance of several density functional theory methods on describing hydrogen-bond interactions. J Chem Theory Comput 5:86–96
29. Riley KE, Pitonak M, Cerny J, Hobza P (2010) On the structure and geometry of biomolecular binding motifs (hydrogen-bonding, stacking, X-H$\cdots\pi$): WFT and DFT calculations. J Chem Theor Comput 6:66–80
30. Bader RFW (1990) Atoms in molecules: a quantum theory. Oxford University Press, Oxford
31. Popelier PLA (2000) Atoms in molecules: an introduction. Prentice Hall, London
32. Matta CF, BR J (2007) The quantum theory of atoms in molecules: from solid state to DNA and drug design. WILEY-VCH, Weinheim
33. Reed AE, Curtiss LA, Weinhold F (1988) Intermolecular interactions from a natural bond orbital, donor-acceptor viewpoint. Chem Rev 88:899–926
34. Reed AE, Weinhold F, Curtiss LA, Pochatko DJ (1986) Natural bond orbital analysis of molecular interactions: theoretical studies of binary complexes of HF, H_2O, NH_3, N_2, O_2, F_2, CO, and CO_2 with HF, H_2O, and NH_3. J Chem Phys 84:5687–5705
35. McLean AD, Chandler GS (1980) Contracted Gaussian basis sets for molecular calculations. I. Second row atoms, Z=11–18. J Chem Phys 72:5639–5648
36. Krishnan R, Binkley JS, Seeger R, Pople JA (1980) Self-consistent molecular orbital methods. XX. A basis set for correlated wave functions. J Chem Phys 72:650–654
37. Boys SF, Bernardi F (1970) The calculation of small molecular interactions by the differences of separate total energies: some procedures with reduced errors. Mol Phys 19:553–566
38. Frisch MJ, Trucks GW, Schlegel HB, Scuseria GE, Robb MA, Cheeseman JR, Scalmani G, Barone V, Mennucci B, Petersson GA, Nakatsuji H, Caricato M, Li X, Hratchian HP, Izmaylov AF, Bloino J, Zheng G, Sonnenberg JL, Hada M, Ehara M, Toyota K, Fukuda R, Hasegawa J, Ishida M, Nakajima T, Honda Y, Kitao O, Nakai H, Vreven T, Montgomery JA, Peralta JE, Ogliaro F, Bearpark M, Heyd JJ, Brothers E, Kudin KN, Staroverov VN, Kobayashi R, Normand J, Raghavachari K, Rendell A, Burant JC, Iyengar SS, Tomasi J, Cossi M, Rega N, Millam JM, Klene M, Knox JE, Cross JB, Bakken V, Adamo C, Jaramillo J, Gomperts R, Stratmann RE, Yazyev O, Austin AJ, Cammi R, Pomelli C, Ochterski JW, Martin RL, Morokuma K, Zakrzewski VG, Voth GA, Salvador P, Dannenberg JJ, Dapprich S, Daniels AD, Farkas Ö, Foresman JB, Ortiz JV, Cioslowski J, Fox DJ (2009) Gaussian 09. Gaussian Inc, Wallingford
39. Biegler-König F (2000) AIM2000, 10th edn. University of Applied Sciences, Bielefeld
40. Benoit DM (2008) Fast vibrational calculation of anharmonic OH-stretch frequencies for two low-energy noradrenaline conformers. J Chem Phys 129:234304
41. Van Mourik T (2005) On the relative stability of two noradrenaline conformers. Chem Phys Lett 414:364–368
42. Van Mourik T, Fruchtl HA (2005) The potential energy landscape of noradrenaline: an electronic structure study. Mol Phys 103:1641–1654
43. Popelier PLA (1998) Characterization of a dihydrogen bond on the basis of the electron density. J Phys Chem A 102:1873–1878
44. Tian SX (2004) Quantum chemistry studies of glycine-H_2O_2 complexes. J Phys Chem B 108:20388–20396
45. Bondi A (1964) van der Waals Volumes and Radii. J Phys Chem 68:441–451
46. Hannachi Y, Silvi B, Bouteiller Y (1992) Ab initio study of the structure, cooperativity, and vibrational properties of the H_2O:$(HF)_2$ hydrogen bonded complex. J Chem Phys 97:1911–1918
47. Mo O, Yanez M, Elguero J (1992) Cooperative (nonpairwise) effects in water trimers: an ab initio molecular orbital study. J Chem Phys 97:6628–6638
48. Frank HS, Wen WY (1957) Ion-solvent interaction. Structural aspects of ion-solvent interaction in aqueous solutions: a suggested picture of water structure. Discuss Faraday Soc 24:133–140
49. Murray JS, Concha MC, Lane P, Hobza P, Politzer P (2008) Blue shifts vs red shifts in sigma-hole bonding. J Mol Model 14:699–704
50. Clark T, Hennemann M, Murray JS, Politzer P (2007) Halogen bonding: the sigma-hole. J Mol Model 13:291–296
51. Murray JS, Lane P, Clark T, Politzer P (2007) Sigma-hole bonding: molecules containing group VI atoms. J Mol Model 13:1033–1038
52. Murray JS, Lane P, Politzer P (2007) A predicted new type of directional noncovalent interaction. Int J Quantum Chem 107 (12):2286–2292
53. Murray JS, Lane P, Politzer P (2008) Simultaneous α-Hole and hydrogen bonding by sulfur- and selenium-containing heterocycles. Int J Quantum Chem 108:2770–2781
54. Murray JS, Lane P, Politzer P (2009) Expansion of the sigma-hole concept. J Mol Model 15:723–729
55. Politzer P, Murray JS, Concha MC (2008) Sigma-hole bonding between like atoms; a fallacy of atomic charges. J Mol Model 14:659–665
56. Politzer P, Murray JS, Lane P (2007) Sigma-hole bonding and hydrogen bonding: competitive interactions. Int J Quantum Chem 107:3046–3052
57. Clark T, Murray JS, Lane P, Politzer P (2008) Why are dimethyl sulfoxide and dimethyl sulfone such good solvents? J Mol Model 14:689–697